Title

A Liquid-Helium-Cooled Absolute Reference Cold Load for Long-Wavelength Radiometric Calibration

Authors

Bensadoun, M
Witebsky, C
Smoot, G
et al.

Publication Date

1990-05-01

LBL-29007
Preprint

Lawrence Berkeley Laboratory
UNIVERSITY OF CALIFORNIA

Physics Division

Submitted to Review of Scientific Instruments

A Liquid-Helium-Cooled Absolute Reference Cold Load for Long-Wavelength Radiometric Calibration

M. Bensadoun, C. Witebsky, G. Smoot,
G. De Amici, A. Kogut, and S. Levin

May 1990

Prepared for the U.S. Department of Energy under Contract Number DE-AC03-76SF00098.

DISCLAIMER

A liquid helium-cooled absolute reference cold load for long-wavelength radiometric calibration

Marc Bensadoun, Chris Witebsky, George Smoot, Giovanni

De Amici, Al Kogut, [a] and Steve Levin

Space Sciences Laboratory and Lawrence Berkeley Laboratory
University of California, Berkeley, California 94720

a)
Laboratory for Astronomy and Solar Physics
NASA / Goddard Space Flight Center, Greenbelt, MD 20771

This work was supported in part by the NSF Division of Polar Programs under Contract No. DPP-8716548, the Physics Division of the Lawrence Berkeley Laboratory, and the Division of High Energy Physics of the U. S. Department of Energy under Contract No. DE-AC03-76SF00098.

A liquid helium-cooled absolute reference cold load for long-wavelength radiometric calibration

Marc Bensadoun, Chris Witebsky, George Smoot, Giovanni De Amici, Al Kogut,[a] and Steve Levin

Space Sciences Laboratory and Lawrence Berkeley Laboratory
University of California, Berkeley, California 94720

a)
Laboratory for Astronomy and Solar Physics
NASA / Goddard Space Flight Center, Greenbelt, MD 20771

ABSTRACT

We describe a large (78-cm) diameter liquid-helium-cooled black-body absolute reference cold load for the calibration of microwave radiometers. The load provides an absolute calibration near the liquid helium (LHe) boiling point, accurate to better than 30 mK for wavelengths from 2.5 to 25 cm (12-1.2 GHz). The emission (from non-LHe temperature parts of the cold load) and reflection are small and well determined. Total corrections to the LHe boiling point temperature are ≤50 mK over the operating range. This cold load has been used at several wavelengths at the South Pole and at the White Mountain Research Station. In operation, the average LHe loss rate was ≤ 4.4 l/hr. Design considerations, radiometric and thermal performance and operational aspects are discussed. A comparison with other LHe-cooled reference loads including the predecessor of this cold load is given.

INTRODUCTION

We have developed a large LHe-cooled cold load (CL) (Figure 1) to permit precise absolute calibration for measurements of the long-wavelength ($\lambda \geq 1$ cm) spectrum of the cosmic microwave background radiation (CMBR). This CL is based on a CL used for the same purpose in 1982-86[1], with improvements derived from our previous experience.

Measurements have been made using this CL at wavelengths of 4.0, 7.9, 12 and 20 cm (7.5, 3.8, 2.5 and 1.5 GHz) in December 1989 from the South Pole and, at all but 12 cm, from the University of California's White Mountain Research Station in September 1988. The results of these measurements are reported by Sironi *et al.*,[2] Kogut *et al.*,[3] and De Amici *et al.*[4] Uncertainty in the CL antenna temperature does not significantly degrade the accuracy of the measurements. Of the South Pole measurements, those at 7.9 and 12 cm were also performed from White Mountain in past years using our previous CL and provide a cross-check of the accuracy of the calibration obtained with the CL described here.

A. SCIENTIFIC CONTEXT

The CMBR is a relic of the early, hot universe whose spectrum contains information on the evolution of the universe. Its spectrum closely approximates that of a blackbody at a temperature of 2.7 K. Spectrum measurements of the Rayleigh-Jeans portion of the CMBR have generally been made with microwave radiometers, devices whose output changes in proportion to the change in input power.[5] The experiment is a measurement of the temperature difference between the sky and the CL. The sky temperature is found by adding the precisely known CL temperature to the measured sky-CL difference. By carefully subtracting any foreground contributions from the sky temperature, one finds the CMBR temperature.

The most accurate measurement is achieved when the CL characteristics are precisely known and most nearly like those of the sky. Radiometer antennas are matched to free-space (in order to observe the sky) and, for $1<\lambda<30$ cm, a radiometer receives 4 to 10 K of effective noise power from the sky. Therefore, the impedance of the CL should be as similar to free space as possible; in particular, the reflection should be small. The cold sky temperature requires a LHe-temperature absorber in the CL. Precise knowledge

of the antenna temperature requires low reflectivity, low emissivity of those parts of the CL not immersed in LHe, and precise knowledge of the physical temperature of the emitter.

Measurements of the CMBR and tests for systematic effects are made from remote, high-altitude sites over a period of several days. Thus, the cold load must be transportable and robust, have stable performance and a low LHe loss rate, even during observations.

I. PREVIOUS COLD LOADS

Long-wavelength measurements of the CMBR have used LHe-cooled waveguide or coaxial cold loads to calibrate. Emission from the antenna and warm parts of such cold loads requires corrections of ~2 K which have been a major source of error (at the ±0.3 K level).[6,7] In the late 1960's, several measurements were made at centimeter wavelengths using LHe-cooled, quasi-free-space waveguide cold loads.[8,9,10] Uncertainty in the cold-load reference was reduced in these experiments to the ±0.1 K level, still a major source of error.

A. The 1982 Cold Load

In 1982, the USA-Italy long-wavelength CMBR collaboration built a large, quasi-free-space-waveguide cold load[1,11] to eliminate the major sources of error present in previous cold loads over the band from 12-0.33 cm. The measurements produced by this collaboration[12] and continued in 1984-7 by the Berkeley group[4,13,14,15] using the 1982 CL were the first for which absolute calibration error was insignificant over the range of 3 to 8 cm. The 1982 CL performance at 12 cm (the design long-wavelength limit) limited the accuracy of the measurement at that wavelength.

The primary features of the 1982 CL were: (1) an absorber (Emerson & Cuming VHP-8 Eccosorb) immersed in LHe with reflection less than 2×10^{-4}, (2) an aluminum-coated (13 μm of Al) mylar radiometric wall (RW) with a diameter of 70 cm diameter, (3) a low-emissivity, boiloff-cooled, manually operated shutter, (4) two 23 μm thick polyethylene windows, and (5) an aluminum interface plate. (Insofar as they exist in the new CL, these elements are indicated in Figure 1.)

In 1986, we made measurements at 21.3 cm, outside the nominal operating range of the cold load. We encountered radiometric problems with the absorber, which was too thin to give low reflection, and with the manually operated shutter near the top of the radiometric wall. Between calibrations the shutter was closed to decrease the radiative heat leak to the cold load; during calibrations the shutter was opened to expose the radiometer to the absorber, but gaps between the shutter and the adjacent radiometric wall gave rise to reflection and emission. Furthermore, the RW was aging and its emissivity could have deteriorated. The heat loads caused by the large antenna and poor dewar vacuum made determination and maintenance of the LHe level very difficult. Consequently, it was decided to build a new cold load with better thermal and operational characteristics and designed specifically for accurate long-wavelength measurements. The 1988 CL described in the present paper is similar in many respects to the 1982 CL and drew extensively on the design, fabrication, operational experience as well as the radiometric performance of the previous effort.

II. COLD LOAD DESIGN AND COMPONENT SELECTION

A. The Absorber

The performance of the absorber at LHe temperatures is the single most important element in the CL. The absorber is characterized by its thermodynamic temperature ($\approx$ 4 K) and its absorption and reflection at the wavelengths of interest at that temperature. The temperature of the LHe bath is very reliably and precisely ($\pm$2 mK) determined via measurement of the pressure over the LHe bath. Electronic sensors embedded in the absorber give a cross-check on the temperature as determined by the pressure measurement.

The primary features sought in the absorber material are good absorption at 4 K, small volume, low specific heat, good porosity, and low cost. The absorber is composed primarily of VHP-12 Eccosorb[16] with a 5.7 cm backing layer of Eccosorb LS-22 and LS-24. Eccosorb is a carbon-impregnated open-cell urethane foam. Physically, the absorber had 25.4 cm high pyramids on an 11.4 cm thick solid base.

Reflection occurs at the front surface of the absorber due to the imperfect dielectric matching of the pyramids to the LHe bath, and at the metal backing. The signal reflected from the metal backing is attenuated by the two-way loss in the absorber. The magnitude of the reflection is determined by the shape of the absorber and the complex dielectric constant, which is temperature and frequency dependent.

As the absorber cools from 300 K to 4 K, reflection from the front surface decreases slightly because the imaginary part of the dielectric constant decreases with temperature. This results in an improved match to the LHe bath; we are not limited by the reflection from the front of the absorber. The decrease in conductivity with temperature (proportional to the imaginary part of the dielectric constant) reduces the loss in the absorber, so more signal passes through it and reflects from the metal backing. At cm wavelengths, the conductivity is only weakly wavelength dependent. This property allows one to scale the absorber dimensions linearly with wavelength to give the same reflection. The measured upper limit on the reflectivity of the 1982 CL with the VHP-8 absorber at 4 K at λ = 12 cm is $r^2 \leq 2 \times 10^{-4}$.[17] We have scaled the absorber thickness to give the same limit on reflectivity at 25 cm wavelength that was previously measured at 12 cm wavelength.

B. Windows

Windows serve two purposes: to prevent condensation from forming on any radiometric surface and to reduce the heat leak to the LHe. The windows are required to have low microwave reflection and emissivity, to be strong enough to support a 4 Torr pressure differential and to withstand mild physical abrasion at temperatures as low as 200 K. The design short-wavelength operating limit affects the window design since windows limit the short-wavelength performance. A window of thickness $t \ll \lambda$ is described by its amplitude reflection r, and emissivity e:

$$r = \pi(\varepsilon - 1)t/\lambda \qquad (1)$$

$$e = \alpha t = 6.30\, t/\lambda\, tan\delta\, \varepsilon^{1/2}\,, \qquad (2)$$

where ε is the dielectric constant, α is the absorption coefficient and $tan\delta$ is the loss tangent of the material. The dependence of both reflection and emission on t requires the windows to be as thin as possible.

We use 23 μm thick polyethylene windows at the top of the CL. Warmed boil-off He gas circulates between the windows to maintain the temperature of the top window above ambient temperature and prevent condensation on any of the radiometric surfaces in the CL.

A 250 K blackbody covering the CL aperture radiates 106 W. If this heat were allowed to reach the LHe bath, it would result in an unacceptable LHe loss rate of 150 l/hr. We reduce the radiative heat leak by the use of infrared (IR) absorbing windows placed just above the LHe bath. The heat absorbed by these windows is removed from the CL by cold He boiloff gas circulating between the windows and then out of the CL. We searched for a glass-Teflon[18] composite material which would exploit the high opacity of glass in the IR, the microwave transparency of both glass and Teflon, and the outstanding flexibility and durability of Teflon at cryogenic temperatures.

We use Fluorglas 381-3[19] cloth to form two windows separated by 5 cm; one layer for the top window, two for the bottom. Fluorglas 381-3 is made by impregnating and coating 1080-style glass cloth with FEP Teflon to a nominal thickness of 75 μm. The material is 30% glass by volume with a total density of 0.0146 g-cm^{-2}. The glass has a dielectric constant $\varepsilon_G \approx 5.0$. We model the Fluorglas as a composite with $\varepsilon_F = \varepsilon_T(1-\delta) + \varepsilon_G\delta \approx 3.0$, where δ is the fraction of glass by volume. The 381-3 fabric is inexpensive, easy to handle and readily available in wide rolls (92 cm).

C. Radiometric Wall

The radiometric wall is an overmoded circular waveguide which links the LHe-temperature absorber to the ambient temperature CL aperture. It extends from the aperture of the CL to the bottom of the absorber. The RW must be cold, have low-emissivity, and subtend a small gain-weighted solid angle, requiring a large diameter RW. The wall must also have low thermal conductivity, be capable of supporting the weight below and have minimal discontinuities. To prevent wrinkling of its surface, we used a rigid backing for the RW. We used two identical 1 mm thick epoxy-fiberglass cylinders lined with 25 μm thick 1100-H19 aluminum (10 skin depths at 1.5 GHz) and left the minimum required space (~1.7 cm) between the RW and dewar walls so as to maximize the RW inside diameter.

Electrical discontinuities were kept to a minimum. Below the Fluorglas windows, there is only one 3.2 mm diameter hole to allow for measurement of the pressure over the LHe bath. There are 32 holes 4 cm above the top Fluorglas window, each 6.4 mm in diameter and backed by copper mesh, spaced evenly around the circumference to allow the He boiloff gas to exit the radiometric space. Close to the top of the upper RW section are a 3.2 mm diameter hole for pressure sensing and a 4.8 mm hole for gas purging. Because the inside diameter of the RW sections is slightly smaller than the nominal 77.74 cm, there is a small step in the diameter (and hence a DC and RF electrical discontinuity) at the joints above and below the Fluorglas window holder, and at the top of the upper RW section. A fourth joint is associated with the DC electrical isolation of the CL from the radiometer interface plates. All four joints have average width of $\leq$0.5 mm and never exceed 1 mm. The leakage and reflection from the joints is minimal. They are not covered by aluminum tape and their contribution to the radiometric temperature is evaluated.

D. Boiloff Helium Flow and Heat Flow

The heat leak to the LHe is minimized by the design of each element. Full advantage is taken of the enthalpy of the He boiloff gas. The gas flow is set up to serve the dual purpose of removing the 50-100 W radiative heat load and keeping the RW and electrical leads as cool as possible. The gas flow is channeled up through holes in the middle of the lower Fluorglas window, out along the outer edge of the upper window, then immediately through the vent holes in the RW and up the annular space between the RW and the dewar wall to 6 vents at the top. The Fluorglas venting cross-section of 16 cm^2 for each window is larger than the RW vent cross-section of 10 cm^2 to prevent any significant flexing or tension. While most of the emerging gas is vented to the atmosphere ~3 m away from the CL, a small fraction is heated and circulated between the polyethylene windows.

E. Sensors and Heaters

Knowledge of the LHe level, pressures throughout the CL and temperature of the absorber, Fluorglas windows and RW are critical to the evaluation of the CL radiometric temperature and to the smooth operation of the CL. The optically opaque Fluorglas windows increase the need for reliable level sensors. In addition, since liquid nitrogen (LN) is used both to precool the CL and for radiometric tests, an LN level sensing system

is necessary. All sensors are placed in the 1.5 cm annular space outside of the RW so as not to affect the radiometric properties of the RW.

Cryogen level is determined by continuous sensors: a 4-wire superconducting sensor (AMI 60 cm) for LHe and a capacitive sensor (Cryomagnetics Model 50) for LN. In addition, ten 330 Ω Allen-Bradley carbon resistors with insulation removed give precise discrete level indication, allow calibration of the continuous sensors, and provide a backup system. The resistors and the LHe continuous sensor are protected from splashing cryogen to improve their stability and reliability.

The discrete level sensor resistors operate at a constant 10 V in order to give good contrast in the resistor current as the liquid level passes the sensor. The current change between liquid and gas (with a change of ~1 mm in cryogen level) is 5 mA to 9 mA for LHe, and 24 mA to 27 mA for LN. The discrete sensors are located in the curvature head and along the continuous sensors and specifically at, and just above, the absorber tips. Although the heat leak produced during the operation of the discrete sensors was small compared to the total heat leak, only one at a time is operated.

Pressures inside the CL are measured via small tubes leading out to differential pressure gauges. The differential pressures across the windows and RW (important because the cryogen level sensors were on the outside of the RW) were measured to better than 0.2 Torr. The differential pressure over the cryogen (compared to ambient) was also measured to ±0.2 Torr, contributing negligibly to the overall uncertainty of the absolute pressure determination (±1 Torr).

The absorber temperature is measured directly by two Lakeshore CGR-1500 carbon-glass resistors (CGR) and one 1N4148 diode. The CGR's have high sensitivity at LHe temperatures and are repeatable, capable of a ±5 mK measurement, while the diode has better sensitivity at near-ambient temperatures to aid in general operation of the CL. The RW temperature is measured to ±5 K by 6 matched 1N4148 diodes epoxied to the exterior of the RW, one below the Fluorglas windows, 5 above.

A 150 W heater at the bottom of the dewar aids in the removal of water vapor, boiling off any LN residue after precooling, and warming up the CL. The dewar heater and the He gas heater are electrically isolated from the CL.

F. Radiometer Interface and Cold Load Cover

Each radiometer achieves a repeatable match to the CL by using a flat interface plate which reduces the CL aperture to match that of the antenna mouth. The details of the interface plate design depend on the radiometer antenna design. The CL itself is electrically isolated from the radiometers by a 0.5 mm layer of epoxy-fiberglass at the CL-radiometer interface.

To further reduce the radiative heat leak and protect the CL during periods between calibrations, a low-emissivity cover is placed over the CL. The lower face of the cover is a layer of aluminized mylar glued to foam insulation.

III. PHYSICAL DESCRIPTION

The 81.3 cm I.D. aluminum/fiberglass vapor-cooled LHe bucket dewar was manufactured by Kadel Engineering. The dewar diameter was set primarily by the sharp increase in cost and weight of LHe bucket dewars with greater diameter. The Al/fiberglass construction was chosen over stainless steel for its lower weight and cost.

The dewar depth is 133 cm. The dewar neck includes two epoxy-reinforced cylinders, each 57 cm long and 1.6 cm thick, with a stainless steel foil He diffusion barrier. The dewar has 5 vapor-cooled radiation shields and multi-layer insulation. Residual gases in the vacuum space are absorbed by 225 g of activated charcoal getter material which is attached to the inner curvature head. The CL is designed to be set up and leveled in a hole with the interface ~3 cm above the level of an observation platform. The overall weight is approximately 350 kg.

With the exception of heaters and three discrete level sensors on the inner curvature head, the radiometric part of the cold load is completely separate from the bucket dewar. The two polyethylene windows are attached to the top and bottom of an aluminum annulus by 0.5 cm thick aluminum rings making gas-tight seals. The window holder is then screwed to the top of the dewar interface making a gas-tight O-ring seal. The dewar

interface holds the RW at its top and also houses the electrical and pressure sensor feedthroughs as well as the vacuum-insulated fill line and gas purge line.

The absorber is backed by copper screen and wedged into the RW. It is held in place by four brackets and by contact at the bottom edge with the dewar. The upper and lower sections of the RW are joined to a three-ring aluminum structure which holds the two Fluorglas windows 5.1 cm apart, and the entire RW is epoxied at the top to the dewar interface. The fill line has a 1.5 m flexible section outside the CL and a rigid section extending to the dewar bottom. The 6 boiloff vent lines extend 15 cm below the dewar flange into the annular space outside the RW to prevent the gas from cooling the interface. The vent line feedthroughs thermally isolate the interface from the cold vent gas. During operation, a 250 W heater keeps the interface at ambient temperature. The two polyethylene windows are held 3.8 cm apart at the edge by the window holder which attaches to the top of the dewar interface. All seals are made gas-tight with O-rings, silicone (for permanent seals) or latex (for the polyethylene windows).

The electronics, meter displays and data recording system were indoors, linked to the CL via several 45 m cables. The He gas pressure and cryogen level sensor readings were displayed on a meter rack near the CL to facilitate filling and general operation, and level and temperature sensors were displayed indoors.

IV. RADIOMETRIC MODELLING

We have modelled the radiometer-CL system as a radiometer observing an ideal absorber, separated by a two-port device with reflection r^2, and loss A. The CL antenna temperature is linearly proportional to the sum of the power emitted by the absorber and attenuated by the lossy elements of the CL, the power emitted from the lossy parts, and the power emitted by the radiometer which is reflected back to the radiometer. By design, the reflection and attenuation are small ($<10^{-3}$) and the emission and reflection terms can be considered independently:

$$T_{A,CL} = T_{A,LHe} + r^2 (T_{B,rad} - T_{A,LHe}) + A (T_{CL} - T_{A,LHe}), \qquad (3)$$

where $T_{A,CL}$ and $T_{A,LHe}$ are the antenna temperatures of the CL and absorber, T_{CL} is the effective physical temperature of the lossy part, and $T_{B,rad}$ is the broadcast temperature of the radiometer.

A. Reflection

The amplitude reflection coefficient r is the coherent sum of the reflections at the absorber, the liquid/gas (LHe/He) interface, the windows, the CL interface and in the radiometer itself. Taking the phase ϕ of the broadcast power reflected back by the radiometer itself as the reference phase, the reflection r as defined in terms of the outgoing electric field amplitude E_o and the reflected electric field amplitude E_r is the sum:

$$r = E_r/E_o = r_R + r_I e^{i\phi I} + r_{P1} e^{i\phi P1} + r_{P2} e^{i\phi P2} + r_{F1} e^{i\phi F1} + r_{F2} e^{i\phi F2}$$

$$+ r_H e^{i\phi H} + r_A e^{i\phi A}, \qquad (4)$$

where the subscripts R, I, P, F, H and A refer to the radiometer, radiometer antenna/CL interface, polyethylene, Fluorglas, LHe/He interface and absorber. P1 and P2 are identical while F2 has twice the thickness of F1. The antenna/CL interface term is generally predicted to be very small ($r \approx 3 \times 10^{-3}$ for the 20 cm wavelength radiometer; see §IV.B) and the term for radiometer-CL interface reflection is dropped in the subsequent analysis. The LHe/He interface reflection is given by $r_H = (\varepsilon_{LHe}-\varepsilon_{He})/(\varepsilon_{LHe}+\varepsilon_{He}) = 1.0 \times 10^{-2}$.

To find the correction due to reflection we compute $|r|^2$. This approach to modelling the CL reflection has the advantage that it gives the phase dependent reflection in addition to the power (phase independent) reflection. This calculation is done in the Appendix.

Two additional factors enter into the calculation of the reflection. Not all of the power reflected reenters the radiometer antenna because the antenna does not, in general, fill the CL aperture and the radiated power diverges according to the field distribution inside the RW. This is expressed by the reflection dilution factor D. The radiation is not monochromatic and so the phase of the reflected signal averages out coherent reflections. The degree to which a coherent reflection term amplitude is reduced is represented by the coherence function C.

The computation gives incoherent (power) reflection terms as well as coherent (amplitude) reflection terms which are summarized in Table 1. The coherent reflection

terms are divided into those dependent on the radiometer position and those independent of the radiometer position. The former group gives the amplitude coefficient of the signal observable by varying the radiometer-CL separation. The latter group depends on the phase relations of the reflections in the CL. Only in the case of the two Fluorglas windows do we know the phase separation. The other terms introduce uncertainty into the estimate of the correction due to reflection.

B. Radiometer-Cold Load Interface Reflection

Special attention was given to the matching between the 20 cm wavelength radiometer and the CL because, at the long-wavelength limit, the approximation to free-space was worst and reflections were the most difficult to measure. We have modelled the radiometer-CL interface by an interface from E-plane corrugated rectangular waveguide to circular guide and did a mode conversion calculation. This approximates the 19°-flare horn antenna by a straight waveguide with only the $H_{1,2}$ fundamental mode propagating.[20] The $H_{1,2}$ field distribution at the interface was matched to the 16 modes with cutoff wavelengths above 20 cm for the 78 cm RW diameter. The amplitudes were determined by calculation of overlap integrals and requiring energy conservation.[21,22]

The results show that the $H_{1,2}$ mode matches very well to the circular guide: the rectangular mode amplitude reflection coefficients are all $< 5 \times 10^{-3}$ and the amplitude reflection of the fundamental is 3×10^{-4}. The modes launched into the circular guide have amplitudes which decrease rapidly with increasing mode number.

The 20 and 12 cm wavelength radiometer antennas are based on the same design. We therefore expect that the matching at 12 cm wavelength is better than at 20 cm. At shorter wavelengths, the free-space approximation is better and we measure the radiometer-CL interface reflection by placing the transition plate over the antenna and observing the signal change. These tests are consistent with no effect at the 25 mK level at 20 and 4 cm wavelengths and no correction has been made.

C. Emission

The CL radiometric temperature is increased by emission from the windows and radiometric wall. A good understanding of these sources of emission is essential since their direct measurement in the CL is not possible. Power emission from the windows in

units of antenna temperature is the product of their emissivity (given in Eq. 2) and temperature.

The RW emission depends on the temperature profile, the surface resistivity, the antenna beam pattern or field configuration and the small gaps in the RW. The Al foil emissivity at 20 cm ($\varepsilon \alpha \lambda^{-1/2}$) varies from 1×10^{-4} at ambient temperature to 4×10^{-5} in LHe, where the temperature dependence was determined from the Gruneisen relation.[23] Emission from a 2.5 μm waxy dielectric coating was included, but contributed negligibly.

We estimate the contribution due to the joints in the RW in the ray approximation and use the amplitude of the emission as the uncertainty to account for the large uncertainty in this calculation. The joint contribution is the integral of the beam times the emission over the wall, using the measured temperature distribution of the wall. At 12 cm, the RW diameter is ~6λ, so the free space approximation is poor but the guide is still highly overmoded. At $\lambda = 20$ cm, a waveguide loss calculation using the mode amplitudes given by the radiometer-CL matching (described in §IV.B) is used to estimate the emission.. The RW emission at 12 cm is interpolated from the 20 cm and 7.9 cm values.

V. MEASUREMENT OF RADIOMETRIC PROPERTIES

We measured the absorber reflection, Fluorglas properties, and the phase-dependent part of the total CL reflection. Our past measurements of the polyethylene window reflection and emission are in agreement with predicted values.

A. Cold Load Reflection

At 20 cm wavelength, we made slotted-line reflection measurements of the CL reflection coefficient with the absorber at ambient and LHe temperatures. There was no measurable change in reflection between ambient and 4 K. The results are plotted in Figure 2 with the reflection from the radiometer viewing the sky. The similarity of the reflection from the CL and sky is confirmation that the CL closely resembles free space. This measured reflection is in agreement with the upper limit specified by the manufacturer. We use the average of the reflection over the bandwidth of the radiometer and take the uncertainty to be ±50%.

Direct measurements of the CL or absorber reflectivity were not made at shorter wavelengths and we use values scaled from the measurement at 20 cm wavelength with an uncertainty of ±50%. The estimated upper limit on absorber reflection as a function of frequency is shown in Figure 3. Values for the radiometers used for the South Pole measurements (including the reflection dilution factor from Table A1) are given in Table 1.

B. Windows

The reflection and emission of the Fluorglas windows at ambient temperature were extensively measured with our radiometers. Because the glass emissivity is expected to drop with temperature, our emission measurements give upper limits on emission in the CL. The ambient microwave properties are in good agreement with published sub-mm measurements.[24]

We measured the emission from ambient temperature Fluorglas material at 20, 7.9, 4.0, 3.0 and 0.33 cm by measuring the signal difference when the material was placed on an aluminum sheet which reflected the radiometer beam to the (cold) sky. The measured absorption coefficient is shown in Figure 4 together with spectrometer measurements at shorter wavelength. We use the extrapolated spectrometer data (which is in good agreement with our measured values) and estimate the uncertainty to be ±50%. Table 2 shows properties of the window materials and the window emissivities.

Combined reflection and emission was measured at the same wavelengths by measuring the signal difference when the Fluorglas was placed over the mouth of the zenith-looking antenna. This does not give a precise measurement of the reflection coefficient because the signal has contributions from emission and coherent reflection which must be removed. Therefore, a direct measurement is necessary. We used a slotted-line reflectometer to measure the power reflectivity of the Fluorglas at 0.91 cm wavelength to be $4\pm1 \times 10^{-4}$. Figure 3 shows this value, the values from measurements made with the radiometers and the average of the value from Eq. 1 and the measurement at 0.91 cm. We take the uncertainty in the Fluorglas reflection coefficient to be ±100%.

C. Radiometer Position-Dependent Reflection

We measure the coherent reflection effect (§IV.A) by varying the radiometer-CL separation. An extension to the RW allows us to vary the radiometer position by $\lambda/2$ to

map out one period of a sine curve. This test has been done at 20, 7.9 and 4.0 cm. The data show no sine curve at any of these wavelengths within the limits of the signal noise. These limits are consistent with theoretical predictions (Table 3).

VI. RADIOMETRIC TEMPERATURE

In this section we evaluate the radiometric temperature of the CL explicitly for the radiometers used at the South Pole in 1989. Emission from the windows and radiometric wall increases the CL radiometric temperature (Figure 5 & Table 4). The temperature of the Fluorglas windows is inferred from the temperature measurements at the wall above and below the windows, typically 50 K and 15 K respectively. We take the upper window to be at 50±10 K, the lower at 25±10 K. The uncertainties in the window temperatures are conservative and take into consideration the efficiency of the convective vapor cooling and possible radiative heating (see §VII.B). The ambient temperature during the measurements at the South Pole is ~250 K.

The RW temperature varies from 50 K just above the Fluorglas windows to 120 K where the He boiloff gas enters the vent tubes (25 cm from the mouth) to 250 K at the mouth. The RW contribution for the South Pole measurements is shown in Figure 5 and Table 4.

Radiation from the annular space between the RW and dewar wall may leak into the radiometric space through the absorber due to improper RF sealing around the absorber. The estimated black body temperature of the annular space is 15±10 K warmer than the LHe bath and thus can increase the radiometric temperature of the absorber. Roughly 50±25 % of the signal will enter into the absorber. The absorber lets 1.0±0.5 % of the signal through at 20 cm and the effective gain-weighted radiating surface is ~9 % of the total absorber area. The attenuation scales exponentially with $1/\lambda$, making the effect most significant at 20 cm. Thus, the contribution is 7±8 mK at $\lambda = 20$ cm and negligible at shorter wavelengths.

The ambient barometric pressure during CMBR measurements ranged from 516 to 523 Torr at the South Pole. The barometric pressure over the LHe bath is increased by 1.0±0.1 Torr due to the slight pressurization in the CL and < 0.1 Torr due to the weight

of the column of cold He gas. The uncertainty in the barometric pressure over the LHe bath during any given measurement was ±1 Torr, dominated by the uncertainty in the measurement of the ambient pressure. The estimated pressure over the LHe bath was 517 - 524 Torr corresponding to a thermodynamic temperature of 3.835 - 3.847 K in the absorber[25] with an uncertainty during any given measurement of ±0.002 K. The CL antenna temperatures during the South Pole measurements are shown in Table 5.

VII. THERMAL PERFORMANCE

A. Liquid Helium Loss Rate

A major success of the CL is its low LHe loss rate. In the absence of the Fluorglas windows, the principal heat leak to the LHe bath is radiative. During calibration, the heat leak would be of order 30 W while, in between calibration when the CL is uncovered the heat leak would be of order 100 W. We predicted the radiative heat leak Q_R with the Fluorglas windows in place by measuring the transmission of the Fluorglas window material at 300 K and 4.2 K from 100 - 1000 cm^{-1} using a Fourier spectrometer. These indicate that the three layers at 300 K and 4.2 K let only 2% or 5% of the power through respectively. Assuming a 250 K greybody with emissivity ε~0.3 at the CL aperture (similar to the 20 cm wavelength radiometer antenna), the radiative heat leak is then $0.6 < Q_R < 1.6$ W. The low-emissivity cover (ε~0.05) at 250 K should give a heat leak of ≤0.25 W. A rough estimate of Q_R is obtained from the total heat leak to the LHe (inferred from the LHe loss rate). The difference between 3.1 W during calibration and 2.2 W with the low-emissivity cover over the aperture is approximately the radiative component. We conclude that, during calibration with the 20 cm wavelength radiometer, $Q_R \sim 0.9$ W, consistent with our predictions.

The remaining heat leak to the LHe bath of 2.2 W comes primarily from conduction down the dewar and radiometric walls. In the absence of any vapor cooling, this heat leak would be ~ 9 W. The heat leak through the dewar vacuum space is <0.1 W. The presence of the Fluorglas windows reduces the convective and conductive heat leak down the He gas column to <0.1 W.

B. Fluorglas Window Temperature

The boiloff gas exits the CL at a temperature of ~120 K when the aperture is covered by the 20 cm wavelength radiometer antenna (the maximum radiative heat leak). From the LHe loss rate and the enthalpy of the exiting boiloff gas, we infer that the gas removes ~88 W of thermal power from the CL. While only ~3 W reaches the LHe bath, the ~35 K temperature drop across the Fluorglas windows (determined from the step in RW temperature) indicates that ~30 W of radiant and convective power is absorbed. The remaining 55 W removed is primarily from vapor cooling of the dewar and radiometric walls.

The heat load to the top Fluorglas window is thus <6 mW-cm^{-2} . The radiative heating of the lower window is 25% that of the upper window and the two-layer lower window is cooled from both sides. Because the heat loading to both windows is small and the boiloff gas is in good contact with the windows, the windows and boiloff gas are in thermal equilibrium. The temperatures used are 50±10 K and 25±10 K for the upper and lower windows respectively.

VIII. OPERATIONAL PERFORMANCE

We prepared the CL for operation by flushing it with dry N_2 gas at a slow rate, changing the volume of gas ~14 times and heating the interior to ~30 C. We then filled the CL with LN to precool it. After several hours, the LN was pumped out through the fill line at a rate of 1 l/min and residual LN in the bottom of the curved dewar bottom was boiled off with the heater. The CL was then purged of the N_2 gas by flowing 7 times the CL volume of dry He gas into the top of the CL while pulling out the colder, heavier N_2 gas via the fill line. As an added precaution, He gas was flowed in the fill line and through the entire system, carefully purging all lines, including the pressure sensing lines.

The LHe transfer required ~15 minutes at a slow rate to cool the dewar bottom, following which the fill rate could be increased to a rate of 3.6 l/min = 0.7 cm/min. Each day, the CL was filled to 15-20 cm above the absorber tips followed by a full day of observations. The level dropped very slowly during observations, less than 0.85 cm/hr.

During observations, the pressure above the LHe bath was <1 Torr above ambient. The top window was periodically checked for frost or debris and cleaned if necessary.

IX. COMPARISON WITH OTHER COLD LOADS

Coaxial cold loads typically have ~300 mK error, even in the same wavelength range as our quasi-free space CL. Previous quasi-free-space cold loads (excepting the 1982 CL) have had larger corrections (and uncertainties) to the LHe bath temperature than the present CL. Table 6 compares four cold loads used for CMBR measurements over the range from ~1-50 cm wavelength. The measurement at 50 cm is that of Sironi *et al.*[26]

The 12 and 7.9 cm wavelength radiometers have made good measurements using the 1982 CL[27,28] and can therefore serve as cross-checks between it and the present CL. Only the 1988 data at 7.9 cm wavelength have been analyzed. Table 7 summarizes the predicted CL temperature, $T_{A,CL}$, and the measured temperatures of the atmosphere, $T_{A,Atm}$, and CMBR, $T_{A,CMBR}$ at 7.9 cm wavelength from 1986-8. The uncertainties are large compared with the uncertainty quoted in this work due to the correction for the atmospheric contribution. Accurate comparison of the cold loads by this method is not possible with the existing data. An accurate comparison of the 1988 CL with the coaxial CL of Limon *et al.* 1989 will be possible from the 1989 South Pole measurements at 12 cm wavelength.[29]

At 7.9 cm wavelength, the CMBR temperatures measured with reference to the two cold loads differ by 161±102 mK, a slight disagreement. If the atmospheric and sky measurements are correct, the difference in measured CMBR temperature from 1986-7 to 1988 is due to the difference in cold loads because the atmosphere was measured independently each year. The determination of the atmospheric contribution introduces an uncertainty of approximately ±50 mK into the data. If the change from 1987 to 1988 was due to the CL used, this implies that the 1982 CL was ~160 mK warmer than the 1988 CL. This cannot be explained by a low 1988 CL temperature since this would require it to be colder than the LHe bath temperature. The 1982 CL could be warmer than predicted if the radiometric properties changed due to repeated use and/or the RW emission was underestimated. The 7.9 cm data imply at least one of the following: 1) the change in the

CL used is the source of the 250 mK change, 2) the 7.9 cm wavelength radiometer had an offset which was dependent on both the year and the radiometer position or load, 3) the atmosphere was ~220 mK warmer in 1988 (but was measured to be ~60 mK warmer). Alternative 3 is inconsistent with atmospheric models and measurements at other wavelengths. We see no evidence to support the second alternative.[4] As discussed above, the design of the 1988 CL eliminates some possible sources of error caused by deterioration in the 1982 CL.

X. CONCLUSIONS

We have shown that over its operating band, the CL very closely approximates the conditions of free space. It has low reflection ($<3.5 \times 10^{-4}$), large diameter (78 cm), and a radiometric temperature very close to that of the sky (difference < 1 K). For the radiometers used at the South Pole in 1989, the total correction to the LHe temperature is <50 mK at 20 cm and <20 mK for $12 > \lambda > 2.5$ cm. The total uncertainty in the radiometric temperature for these radiometers is <25 mK for $20 > \lambda > 2.5$ cm.

The thermal characteristics allow day-long periods of operation without a LHe fill. The boiloff rate is not strongly dependent on the radiative load at the aperture, giving very stable operation and radiometric performance.

Several improvements could easily be made. The back of the absorber should be completely closed, allowing no path for radiation to enter from outside the RW. The joints in the RW should be covered or eliminated. The glass-Teflon IR-blocking material would perform better both in the IR and microwave if the glass were quartz and if, instead of a woven fabric, the glass were a thin film. Any future measurement should include direct measurement of the reflection from the radiometer antenna, the radiometer-CL interface plate and the CL, similar to that made with the 20 cm wavelength radiometer.

This CL could be used at ~ 30 cm wavelength if a thicker absorber were used. To be useful at yet longer wavelengths, this CL design would have to be modified so as not to use a prohibitive volume of LHe. To be useful at shorter wavelengths, a better IR-blocking material must be used or a higher heat leak to the LHe bath tolerated. The corrections due to

the windows and warm parts of the CL would be reduced by cooling the whole experiment and operating at balloon altitudes.[30]

ACKNOWLEDGEMENTS

We thank John Gibson for the electronics in the CL, the Mechanical Shops at LBL, in particular Armando Meuti and Kit Mui for their help in manufacturing parts of the CL, Keith Alexander at Kadel Engineering, David Miller and Bob McMurray for their help in the measurement of the IR properties of Fluorglas, and Scott Friedman for work on the 1982 CL. We also gratefully acknowledge the assistance of Barron Chugg, Jenny Hwang, Jay Levin, Michele Limon, and Faye Mitschang. This work was supported by the NSF Division of Polar Programs under Contract No. DPP-8716548, the Physics Division of the Lawrence Berkeley Laboratory, and the Division of High Energy Physics of the U.S. Department of Energy under Contract No. DE-AC03-76SF00098.

APPENDIX

Following the definitions of §IV.A, we explicitly compute the CL reflection coefficient:

$$
\begin{aligned}
|r|^2 = {} & r_R^2 + 2r_P^2 + r_{F1}^2 + r_{F2}^2 + r_H^2 + r_A^2 \\
& + 2r_R r_P \cos(\phi_{P1}) + 2r_R r_P \cos(\phi_{P2}) + 2r_R r_{F1} \cos(\phi_{F1}) + 2r_R r_{F2} \cos(\phi_{F2}) \\
& + 2r_R r_H \cos(\phi_H) + 2r_R r_A \cos(\phi_A) + 2r_P^2 \cos(\phi_{P2} - \phi_{P2}) \\
& + 2r_{F1} r_{F2} \cos(\phi_{F1} - \phi_{F2}) + 2r_{F1} r_H \cos(\phi_{F1} - \phi_H) + 2r_{F1} r_A \cos(\phi_{F1} - \phi_A) \\
& + 2r_{F2} r_H \cos(\phi_{F2} - \phi_H) + 2r_{F2} r_A \cos(\phi_{F2} - \phi_A) + 2r_H r_A \cos(\phi_H - \phi_A). \qquad \text{(A1)}
\end{aligned}
$$

The r_R^2 term is a correction to the radiometer gain and broadcast temperature and does not affect the CL temperature or the measurement.

The reflection dilution factor D, calculated in the ray approximation, is the fraction of power broadcast which reenters the antenna aperture. This factor applies to all terms and for the longest wavelength radiometers, D ~ 1.

The phase-dependent terms represent reflected signals from two points arriving at the first amplifier with correlated phases. The path length between the sources of reflection and the radiometer bandwidth determine the degree of coherence, which averages out these phase-dependant terms by an amount C(z). To evaluate this function, we approximate the bandpass as square and for separations of greater than 1/4 coherence length, the envelope of the coherence function is used:

$$
\begin{aligned}
C(z_{a,b}) &= \left(\frac{\sin(z)}{z}\right)^2 \quad \text{for } z < \frac{\pi}{2} \\
&= \left(\frac{1}{z}\right)^2 \quad \text{for } z > \frac{\pi}{2}, \qquad \text{(A2)}
\end{aligned}
$$

where $z_{a,b} = 2\pi x/L$, x is the separation between the two reflections a and b (half the path length) and $L = c/\Delta\nu$ is the coherence length in terms of the speed of light c and the bandwidth $\Delta\nu$.

The CL reflection coefficient is then:

$$
\begin{aligned}
|r|^2 = {} & 2r_P^2 + r_{F1}^2 D_{F1} + r_{F2}^2 D_{F2} + r_H^2 D_H + r_A^2 D_A \\
& + 2r_R r_{P1} \cos(\phi_{P1})\, C(z_{R,P1}) + 2r_R r_{P2} \cos(\phi_{P2})\, C(z_{R,P2}) \\
& + 2r_R r_{F1} \cos(\phi_{F1})\, D_{F1}\, C(z_{R,F1}) + 2r_R r_{F2} \cos(\phi_{F2})\, D_{F2}\, C(z_{R,F2}) \\
& + 2r_R r_H \cos(\phi_H)\, D_H\, C(z_{R,H}) + 2r_R r_A \cos(\phi_A)\, D_A\, C(z_{R,A}) \\
& + 2r_{F1} r_{F2} \cos(\phi_{F1} - \phi_{F2})\, D_{F1}\, C(z_{F1,F2}) \\
& + 2r_{F1} r_H \cos(\phi_{F1} - \phi_H)\, D_{F1}\, C(z_{F1,H}) \\
& + 2r_{F1} r_A \cos(\phi_{F1} - \phi_A)\, D_{F1}\, C(z_{F1,A}) \\
& + 2r_{F2} r_H \cos(\phi_{F2} - \phi_H)\, D_{F2}\, C(z_{F2,H}) \\
& + 2r_{F2} r_A \cos(\phi_{F2} - \phi_A)\, D_{F2}\, C(z_{F2,A}) \\
& + 2r_H r_A \cos(\phi_H - \phi_A)\, D_H\, C(z_{H,A}) \\
& + 2r_P^2 \cos(\phi_{P1} - \phi_{P2})\, D_{P1}\, C(z_{P1,P2}) \qquad \text{(A3)}
\end{aligned}
$$

The first five terms in Eq. A3 are phase-independent terms and are calculated from measured and predicted reflection coefficients. Terms 6-11, the coherent reflection terms, are dependent on the distance between the radiometer and the CL and are proportional to the reflection coefficient of the radiometer. We use the linear sum of the coherent terms to estimate the magnitude of the coherent reflection effect. Because the phase difference between the radiometer and CL is unknown, we average over the phase; this multiplies the coherent terms by a factor of 0 ± 0.7. This estimate of the error due to coherent reflection is conservative because we have used the linear sum whereas some of the terms could have opposite sign and partially cancel each other. Note that each term in the sum has a large uncertainty due to our poor knowledge of r_R; we estimate this error as $\pm r_R$.

The last seven terms (12-18) are dependent on the separations between the reflecting surfaces within the CL. In the case of the Fluorglas windows, the actual phase of the reflection is known but the separation could change by ± 1 cm due to flow of the He gas. Our best estimate of this term is included as a correction and 50% of this term is included in the calculation of the uncertainty of incoherent reflection.

The last six terms (13-18) depend on separations which are not well known. The phase of the polyethylene window reflection varies, as does that of the LHe/He interface. The phase of the reflection from the absorber reflection is unknown. Because the phase uncertainties are large and uncorrelated, we use 0.7 times the quadrature sum of terms 13-18 as a contribution to the incoherent reflection uncertainty. For the radiometers used at the South Pole in 1989, Table A1 shows some of the radiometer parameters which enter into Eq. A3 and Table 2 shows the values of the resulting terms.

TABLE 1. Reflection Term Coefficients Contributing to r^2. Term numbers refer to Eq 5. We approximate D_A by D_H. The coherent reflection effect amplitude is 0.7 of the sum of Terms 6-11 and gives the predicted amplitude coefficient of the coherent reflection effect obtained by varying the radiometer-CL separation. The position-independent F1-F2 coherent term (Term 12) is known and is used as a correction. The position-independent coherent reflection is the quadrature sum of Terms 12-18; these terms are all independent of radiometer position. To get effect in K, multiply by T_B-T_{LHe} from Table A1.

λ (cm)	20	12	7.9	4.0
	[10^{-5}]	[10^{-5}]	[10^{-5}]	[10^{-5}]
$2r_P^2$	0.041	0.11	0.26	1.0
$(r_{F1}^2 + r_{F2}^2)\, D_F$	0.96	4.1	4.4	2.9
$r_H^2\, D_H$	11	11	2.5	0.54
$r_A^2\, D_H$	35	10	0.92	0.050
Coherent reflection effect amplitude	16	17	20	4.5
Position-independent F1-F2 coherent	-0.75	+1.9	-0.9	-2.1
Position-independent coherent	24	15	3.6	0.68

TABLE 2. Window Material Properties and Emissivities. Emissivities are for the indicated thickness of material. α for glass is from extrapolation of published data and measured values. The data for glass at 290 K give upper limits on the emissivity at lower temperature. The error on the polyethylene and glass emissivities are 33% and 50% respectively.

Material	Material Properties				Window Emissivity			
	ε	tanδ	α (cm^{-1})	t	20 cm	12 cm	7.9 cm	4.0 cm
		(10^{-4})	(10^{-4})	(μm)	(10^{-6})	(10^{-6})	(10^{-6})	(10^{-6})
Polyethylene	2.26	3 to 6		23	0.49	0.81	1.2	2.4
TFE Teflon	2.08	4		25	0.46	0.77	1.2	2.3
glass (290K)	5.9		7.1	50	3.6			
			16	50		8.1		
			31	50			16	
			93	50				47

TABLE 3. Coherent Reflection Test Summary. Predicted amplitude is from Tables 1 and 2 where the uncertainty reflects the factor of two uncertainty in r_R. All measurements give only upper limits on the effect. No measurement was made at 12 cm wavelength.

λ (cm)	20	12	7.9	4.0
	(mK)	(mK)	(mK)	(mK)
Predicted amplitude	8±16	2±4	12±23	7±14
Measured upper limit	0±14	---	0±30	0±21

TABLE 4. Emission from Windows and RW Data from Table 2. Fluorglas emission is for 50 μm of glass and 25 μm FEP Teflon per layer. RW emission is from mode loss calculation for 20 cm radiometer, and from beam integration for 7.9 and 4.0 cm. The contribution from joints is listed separately. Value at 12 cm is interpolated.

Source	T	20 cm	12 cm	7.9 cm	4.0 cm
	(K)	(mK)	(mK)	(mK)	(mK)
Polyethylene (2)	250±10	0.3±0.1	0.4±0.1	0.6±0.2	1.2±0.5
Top Fluorglas	50±10	0.2±0.1	0.4±0.2	0.8±0.3	2.2±0.9
Bottom Fluorglas	25±10	0.2±0.1	0.4±0.3	0.8±0.3	2.2±1.3
RW (w/out joints)	4-250	4±4	2±2	0±1	0±1
RW joints	30-250	13±13	7±7	2±2	2±2
Absorber Leakage	20±10	7±7	0.7±0.8	0	0
Total Emission		25±16	11±7	5±3	8±3

TABLE 5. Cold Load Antenna Temperature. Values are for Radiometers used at the South Pole in December 1989 for pressure over the LHe bath of 520 Torr and a corresponding temperature of 3842 mK. The absorber leakage is included in RW emission. Total Correction plus Absorber Emission gives CL Antenna Temperature.

λ (cm)	20	12	7.9	4.0
	(mK)	(mK)	(mK)	(mK)
Absorber Emission	3806±2	3782±2	3752±2	3665±2
Window Emission	1±1	1±1	2±1	6±2
RW Emission	24±16	10±7	2±2	2±2
Incoherent Reflection	23±15	7±4	6±5	7±9
Coherent Reflection	0±8	0±5	0±18	0±13
Total Correction	48±23	18±10	10±18	15±16
CL Antenna Temperature	3854±23	3801±10	3762±19	3679±16

TABLE 6. Comparison of Cold Loads Used for Long-Wavelength Measurements of the CMBR. Characteristics are given at wavelengths of observations. r^2 is the incoherent (power) reflection coefficient. Subscripts RW and W designate the radiomtric wall and windows respectively. The total correction to the LHe temperature is given by T_{CORR}. Values are from Table 5 for 'this work'. When the design required a break in the horn, the correction for emission from the removable part is given by T_{Horn}.

Measurement	λ	r^2	$r^2T_{B,rad}$	$e_{RW}T_{RW}$	e_WT_W	T_{CORR}	T_{Horn}[a]
	(cm)	(10^{-4})	(mK)	(mK)	(mK)	(mK)	(mK)
Sironi *et al.* 1990a[b]	50	13±3	455±105	1450±280	0	1900±300	1550±130
	12	28±3	140±15	4760±300	0	4800±300	†
this work	20	4.7	26±19	31±19	1±1	58±28	---
	12	2.3	4±3	10±7	2±1	15±8	---
	7.9	4.1	5±4	2±2	2±1	10±12	---
	4.0	2.3	6±3	2±2	7±4	15±8	---
Stokes *et al.* 1967[c]	3.2	6±3	20±10	160±100	60±20	240±100	[d]
	1.58	10±3	30±10	210±80	40±10	280±80	3
Wilkinson 1967[c]	0.856	0±3	0±10	280±110	60±60	340±125	---
Johnson and Wilkinson 1987[e]	1.2	5	0±18[f]	0	35±12[g]	35±22	50±12

[a] '---' indicates that the calibration was at the horn aperture

[b] coaxial CL reference used is that described in Limon *et al.* 1989. These measurements were conducted in 1988 at Alpe Gera, Italy. The 12 cm wavelength radiometer did not make CMBR observations in 1988, but is the same instrument as that used in 'this work' but used the coaxial CL.

[c] the measurements at 3.2, 1.58 and 0.856 cm used the same CL

[d] no value for this quantity is given

[e] CL is an integral part of the radiometer

[f] difference in horn and CL reflection using conservative error bars added in quadrature

[g] window is viewed during sky observation and not during CL calibration

† no value is yet available

TABLE 7. Comparison of CMBR Measurements Made with the 1982 CL and 1988 Cold Loads

λ (cm)	8.1[a]	7.9	7.9
year	1986	1987	1988
predicted $T_{A,CL}$	3735±55	3742±38	3697±21
$T_{A,Atm}$	870±108	898±64	955±55
$T_{A,CMBR}$	2580±130	2460±79	2621±65

[a] radiometer center wavelength was changed from 8.1 cm in 1986 to 7.9 in 1987; the bandwidth was also changed, from 460 MHz to 200 MHz which increased the amplitude of the coherent reflection terms for this radiometer.

TABLE A1. Radiometer Dependent Reflection Coefficient Parameters in Eq 5. r_R^2 has a factor of 2 uncertainty. For reflection dilution factors $D_A \sim D_H$ and $D_F \equiv D_{F1} \sim D_{F2}$. $C(z_{F1,F2}) \sim 1$ and terms like $C(z_{R,H})$ depend on the LHe level.

λ (cm)	20	12	7.9	4.0
r_R^2	0.01	0.01	0.1	0.01
L (cm)	150	187	150	60
T_B-T_{LHe} (K)	50	27	86	279
D_F	1	1	0.46	0.079
D_H	1	1	0.23	0.050
$C(z_{R,F})$	0.044	0.045	0.026	0.0074
$C(z_{R,H})$	0.025	0.028	0.017	0.0042
$C(z_{F,H})$	0.44	0.60	0.44	0.071
$C(z_{F,A})$	0.22	0.34	0.22	0.035
$C(z_{H,A})$	0.87	0.92	0.87	0.39

a) Present address: Laboratory for Astronomy and Solar Physics, Code 685.3, NASA Goddard Space Flight Center, Greenbelt, MD 20771.

1 G. Smoot, *et al. Phys. Rev. Letters*, **51**, 1099 (1983).

2 G. Sironi, *et al.*, to be submitted (1990).

3 A. Kogut, M. Bensadoun, G. De Amici, S. Levin, G.F. Smoot, and C. Witebsky, Ap. J. , (May issue) in press (1990).

4 G. De Amici, M. Bensadoun, M. Bersanelli, A. Kogut, S. Levin, G. Smoot, and C. Witebsky, Ap. J., (Aug 10 issue) in press (1990).

5 This measures power in units of antenna temperature T_A which is related to the thermodynamic temperature T of the source by $T_A = T\,x\,(e^x - 1)^{-1}$, where $x = h\nu/kT$. Over the operating range of the CL, $T_A \approx T$.

6 M. Limon, C. Marchioni, and G. Sironi, J. Phys. E. Sci. Instrum. (UK), **22**, 963 (1989).

7 For a review of all measurements up to 1980, see R. Weiss, Ann. Rev. Ast. Ap., **18**, 489 (1980).

8 R.A. Stokes, R.B. Partidge, and D.T. Wilkinson, Phys. Rev. Lett., **19**, 1199 (1967).

9 M.S. Ewing, B.F. Burke, and D.H. Staelin, Phys. Rev. Lett., **19**, 1251 (1967).

10 D.T. Wilkinson, Phys. Rev. Lett., **19**, 1195 (1967).

11 C. Witebsky, Ph. D. Thesis, Dept. of Astronomy, U.C. Berkeley (1985).

12 G. Smoot, *et al.*, Ap. J. Lett., **291**, L23 (1985).

13 G.F. Smoot, M. Bensadoun, M. Bersanelli, G. De Amici, A. Kogut, S. Levin, and C. Witebsky, Ap. J. Lett., **317**, L345 (1987).

14 M. Bersanelli, C. Witebsky, M. Bensadoun, G. De Amici, A. Kogut, L. Levin, and G. Smoot, Ap. J., **339**, 632 (1989).

15 A. Kogut, M. Bersanelli, G. De Amici, S.D. Friedman, M. Griffith, B. Grossan, S. Levin, G.F. Smoot, and C. Witebsky, Ap. J. **235**, 1 (1988).

16 Eccosorb is manufactured by Emerson & Cuming

17 G. Sironi, private communication (1988).

18 Teflon is manufactured by DuPont

19 Manufactured by Fluorglas, a division of Allied Signal

20 C. Witebsky, G.F. Smoot, S. Levin, and M. Bensadoun, IEEE Antennas and Propagation, **AP-35**, 1310 (1987).

21 A. Wexler, IEEE Trans. on Microwave Theory and Techniques, **MTT-15**, 508 (1967).

22 M.S. Narasimhan and V. Venkateswara Rao, IEEE Antennas and Propagation, **AP-21**, 320 (1973).

23 J. Bardeen, J. Appl. Phys. 11, 88 (1940).

24 M. Halpern, H.P. Gush, E. Wishnow, V. De Cosmo, Appl. Optics, **25**, 565 (1986).

25 M. Duriex and R.L. Rusby, Metrologia, **19**, 67 (1983).

26 G. Sironi, M. Limon, G.L. Marcellino, G. Bonelli, M. Bersanelli, G. Conti, and K. Reif, Ap. J., (July 10 issue) in press (1990).

27 G. Sironi and G. Bonelli, Ap. J., **311**, 418 (1986).

28 G. De Amici, G. Smoot, J. Aymon, M. Bersanelli, A. Kogut, S. Levin, and C. Witebsky, Ap. J., **329**, 556 (1988).

29 G. Sironi, private communication (1990).

30 D.G. Johnson and D.T. Wilkinson, Ap. J. (Letters), **313**, L1 (1986).

Figure captions

FIGURE 1. Cross-sectional schematic of the cylindrical cold load. The He boiloff gas flows through holes in the Fluorglas windows (as indicated), then through the RW, up the annular space (not shown) and out the vents. The location of several of the discrete level sensors and temperature sensors are indicated by **L** and **T** respectively. The resistive heater at the bottom of the CL is shown. The Fluorglas windows of the present CL replace a manually operated shutter which was located just below the polyethylene windows of the 1982 CL.

FIGURE 2. Cold load reflection at 20 cm wavelength. The measurement was made with a slotted line inserted between the radiometer horn and waveguide-coaxial transition. Sky reflection is shown for reference. No change in the CL reflection is observed between ambient and LHe temperature absorber.

FIGURE 3. Absorber and window power reflection coefficients. The absorber used has additional backing and lower reflection than the manufacturer's specified upper limit for VHP-12. The value at 20 cm is a result of the measurement in Figure 2. Measured values are shown for a single thickness (68 μm) of Fluorglas and the model (the value used in the analysis) is the average of the theoretically predicted value and the measured value at 0.91 cm wavelength. The uncertainty used for the Fluorglas reflection is indicated. Reflection from a single layer of 23 μm polyethylene is shown.

FIGURE 4. Absorption coefficient of Fluorglas. The radiometer data agree with the Pyrex data for $0.03 < \lambda < 0.3$ of Halpern *et al.* and their best fit parameters are used with an uncertainty of ±50% as indicated on the long-wavelength extrapolation. This uncertainty allows for a decrease in the absorption as the Fluorglas cools.

FIGURE 5. Emission from windows and radiometric wall. Values are for the observed RW temperature profile. The upper and lower Fluorglas windows are at 50±10 and 25±10 K respectively; the polyethylene windows are at 250±10 K. The radiometric wall data is calculated.

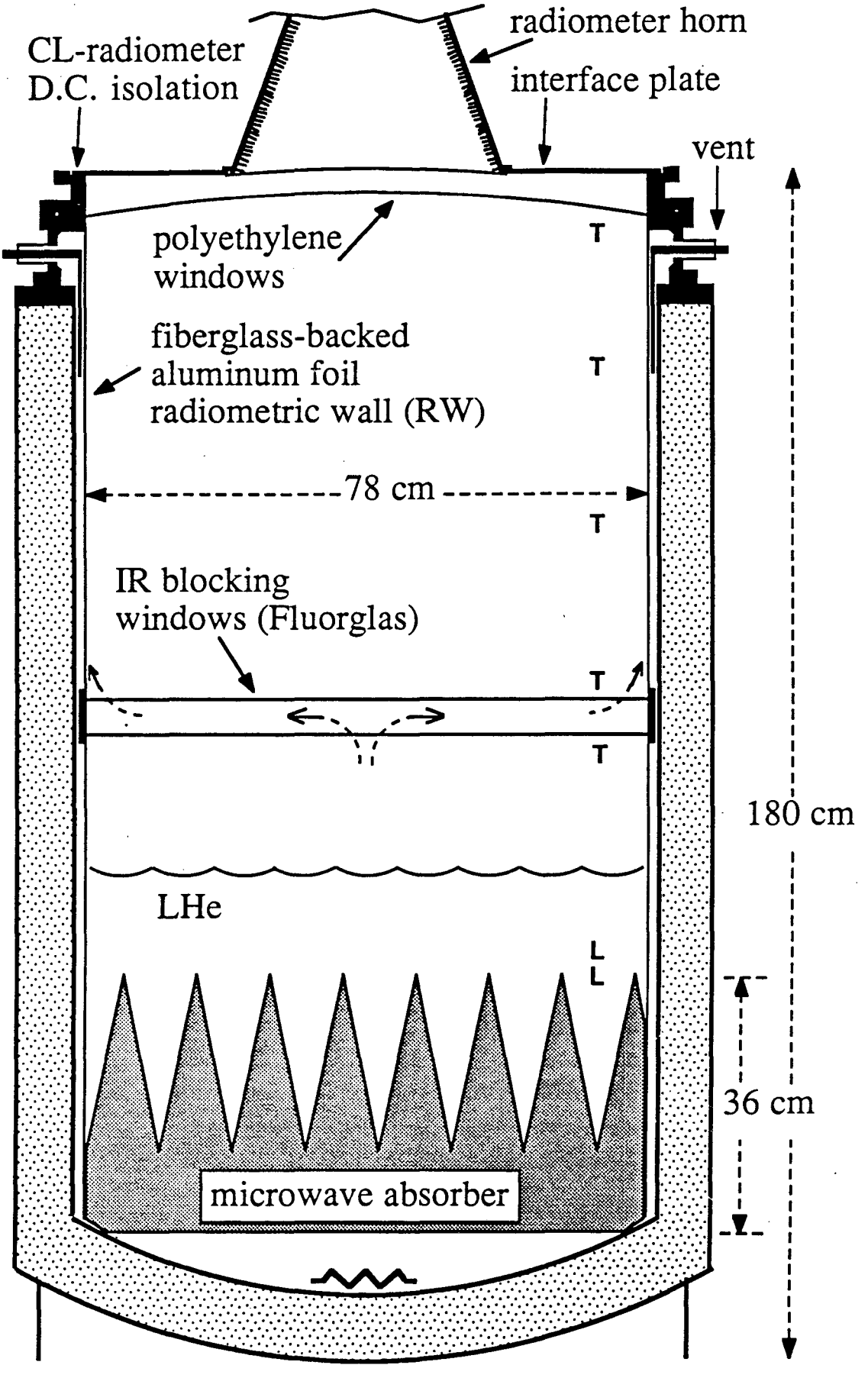
CL-radiometer
D.C. isolation
radiometer horn
interface plate
vent
polyethylene
windows
fiberglass-backed
aluminum foil
radiometric wall (RW)
78 cm
IR blocking
windows (Fluorglas)
T
T
T
T
T
T
LHe
L
L
180 cm
36 cm
microwave absorber

Figure 1.

Figure 2

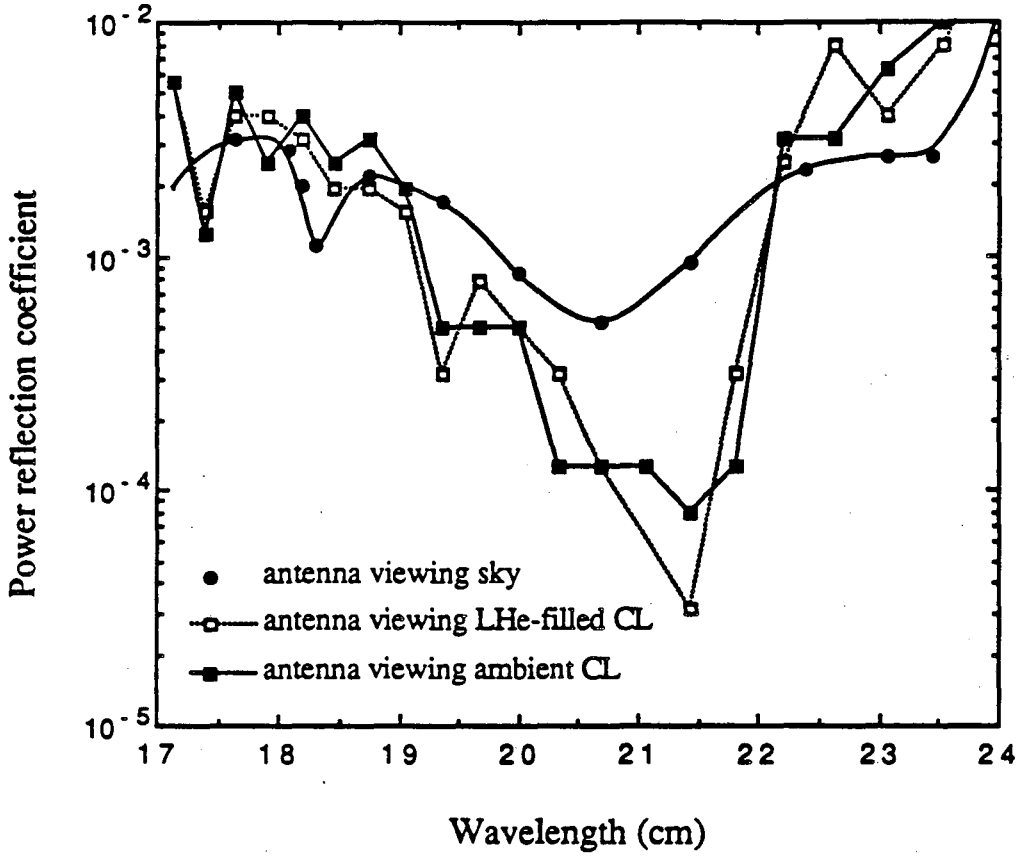

Figure 3

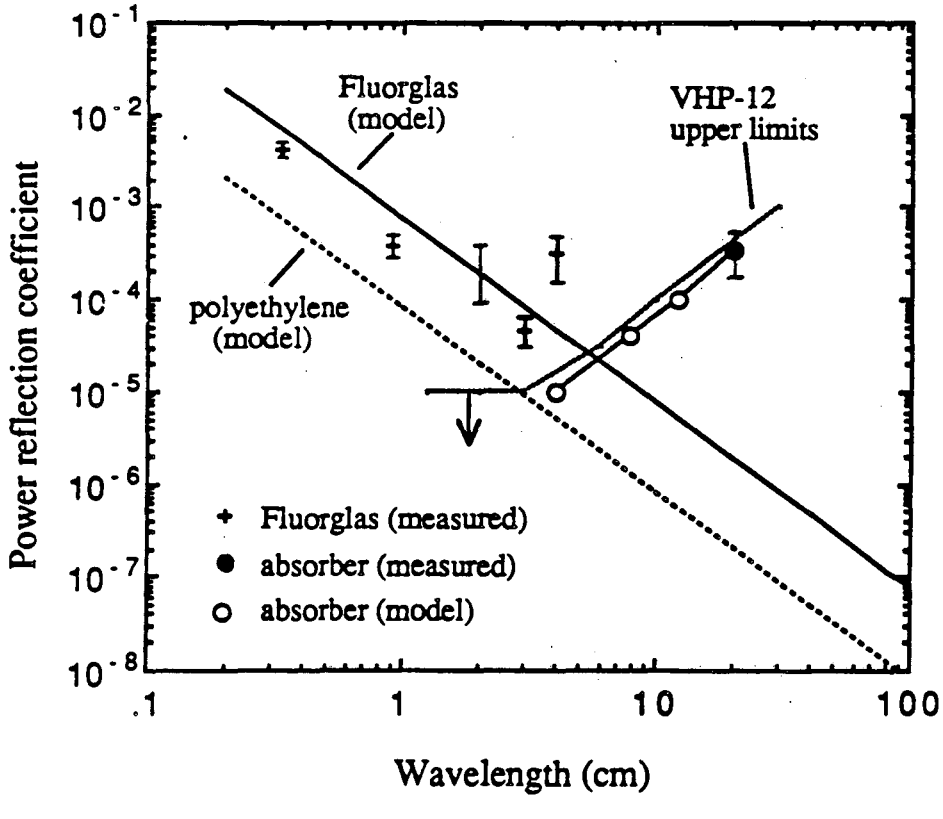

Figure 4

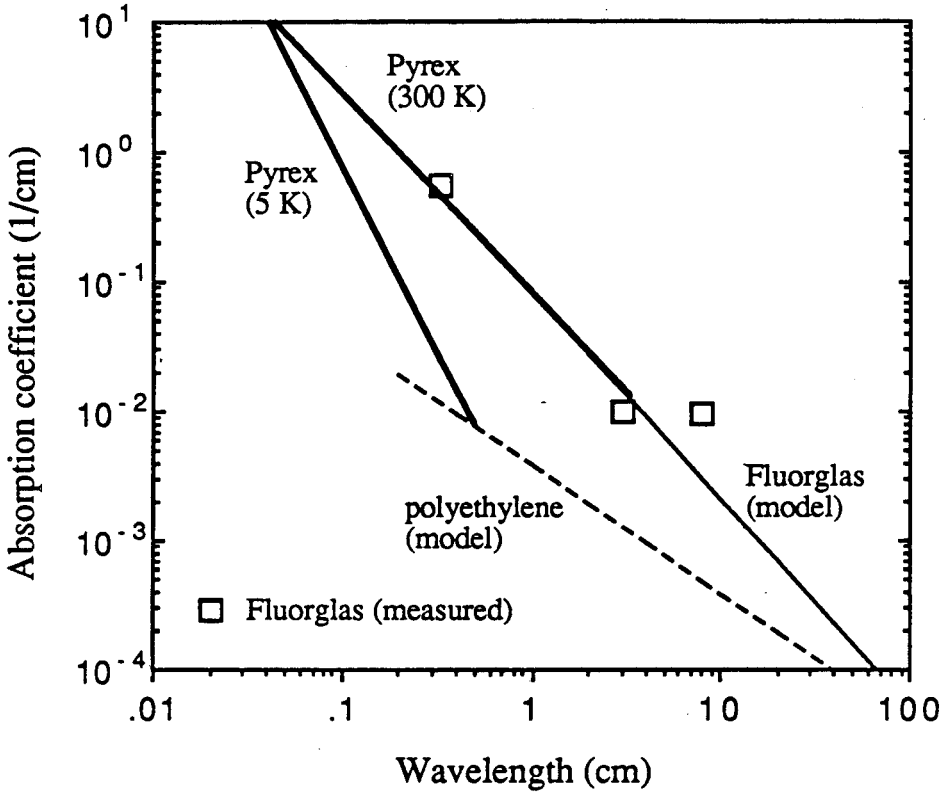

Figure 5

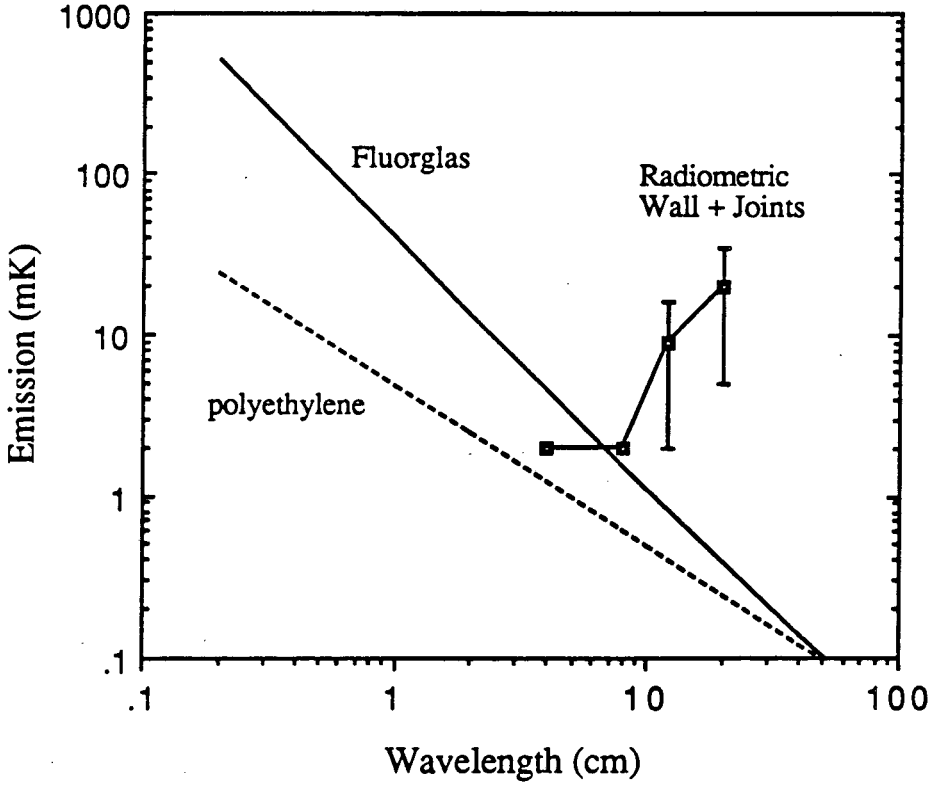

LAWRENCE BERKELEY LABORATORY
UNIVERSITY OF CALIFORNIA
INFORMATION RESOURCES DEPARTMENT
BERKELEY, CALIFORNIA 94720